

## Article

# An Efficient Approach for Lithium and Aluminum Recovery from Coal Fly Ash by Pre-Desilication and Intensified Acid Leaching Processes

Shenyong Li , Shenjun Qin \*, Lianwei Kang, Jianjun Liu, Jing Wang and Yanheng Li

Key Laboratory for Resource Exploration Research of Hebei Province, Hebei University of Engineering, Handan 056038, China; shenyong360@hebeu.edu.cn (S.L.); kanglianwei@126.com (L.K.); liujianjun1060@hebeu.edu.cn (J.L.); wangjing081824@126.com (J.W.); liyh1982@gmail.com (Y.L.)

\* Correspondence: qinsj528@hebeu.edu.cn; Tel.: +86-0310-857-7902

Received: 26 June 2017; Accepted: 11 July 2017; Published: 14 July 2017

**Abstract:** A novel technique was developed for the recovery of lithium and aluminum from coal fly ash using a combination of pre-desilication and an intensified acid leaching process. The main components of the high-aluminum fly ash were found to be  $\text{Al}_2\text{O}_3$  and  $\text{SiO}_2$ , and the Al/Si ratio increased from 1.0 to 1.5 after desiliconization. The lithium content of the coal fly ash met national recycling standards. The optimal acid leaching conditions, under which the leaching efficiencies of lithium and aluminum were 82.23% and 76.72%, respectively, were as follows: 6 mol/L HCl, 1:20 solid to liquid ratio, 120 °C and 4 h. During the hydrochloric acid pressure leaching process, spherical particles of desilicated fly ash were decomposed into flakes. Part of the mullite phase was dissolved, and most of the glass phase leached into the liquor. The generation of the silicates hindered lithium transport, which decreased the leaching rate of lithium. This work suggests that the preprocessing is a promising option for effective recovery of high-aluminum and fly ash-associated lithium.

**Keywords:** coal fly ash; pre-desilication; acid leaching; lithium; high-aluminum

## 1. Introduction

Coal fly ash (CFA) is an industrial waste residue formed from organic matter, clay, and associated minerals after the high-temperature combustion and cooling of coal in coal-fired power plants. CFA can cause serious dust pollution [1], and the toxic elements contained in CFA can leach into soil and cause serious secondary pollution [2–4]. Millions of tonnes of CFA, containing high proportions of aluminum and lithium, are released each year from coal-fired power stations in the Inner Mongolia, Ningxia, and Shanxi provinces in northern China [5–8], which is illustrated in Figure 1. Typically, the CFA in these areas contains 40–50% aluminum and more than 0.2% lithium. The lithium content of this CFA generally exceeds the comprehensive industrial recycling index of the Chinese national standard for Specifications for Rare Metal Mineral Exploration (DZ/T/0203-2002) regarding pegmatite-associated lithium. Considering its high aluminum and lithium content [5,9], this CFA can be utilized as a substitute for bauxite and allophyltin, high quality sources of which are scarce in China. The fly ash covered in this study was markedly enriched in a number of trace elements in comparison with that of the other regions shown in Figure 2 [10,11]. Furthermore, the lithium contained in the CFA should be recycled. Therefore, the development of an effective extraction technique for aluminum and lithium from CFA is of great significance to resources recycling [12].

Previously, aluminum has been recovered from CFA using hydrometallurgy techniques such as solvent extraction [13], acid leaching [14–18], alkaline leaching [19–21], and acid/alkali combination methods [22]. The CFA may be pre-processed before leaching using auxiliary reinforcement methods, such as lime stone sintering [6], soda lime sintering [23], and ammonium sulfate sintering [14,24].

Each process has its own advantages and disadvantages. For instance, large quantities of residue (8–10 times greater than the original quantity of CFA) are generated during sintering [25]. Moreover, ammonium sulfate sintering also produces toxic gases, such as ammonia. Alkaline leaching requires more energy and material than acid leaching, and exhibits a lower aluminum extraction efficiency. With the development of corrosion-resistant materials, acid leaching has become increasingly feasible and efficient. However, CFA contains various minerals that are not readily dissolved in solutions of mineral acids, such as mullite, quartz, alpha-aluminum, and aluminosilicate. Hence, the direct acid leaching of CFA is impracticable, and destroys the structure of the CFA. The addition of fluoride can significantly improve the acid leaching of CFA [18]. Moreover, a mixture of ammonium bisulfate and aqueous sulfuric acid was used for the high-efficiency leaching of aluminum from high-aluminum CFA [14]. However, these techniques consume large quantities of acid and cause secondary pollution.

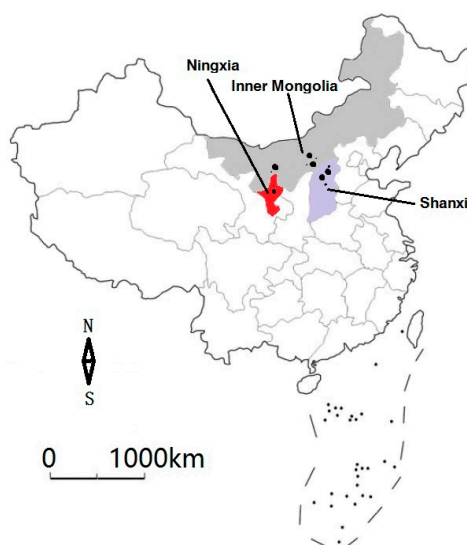


**Figure 1.** Location of the high-aluminum coalfields in northern China.

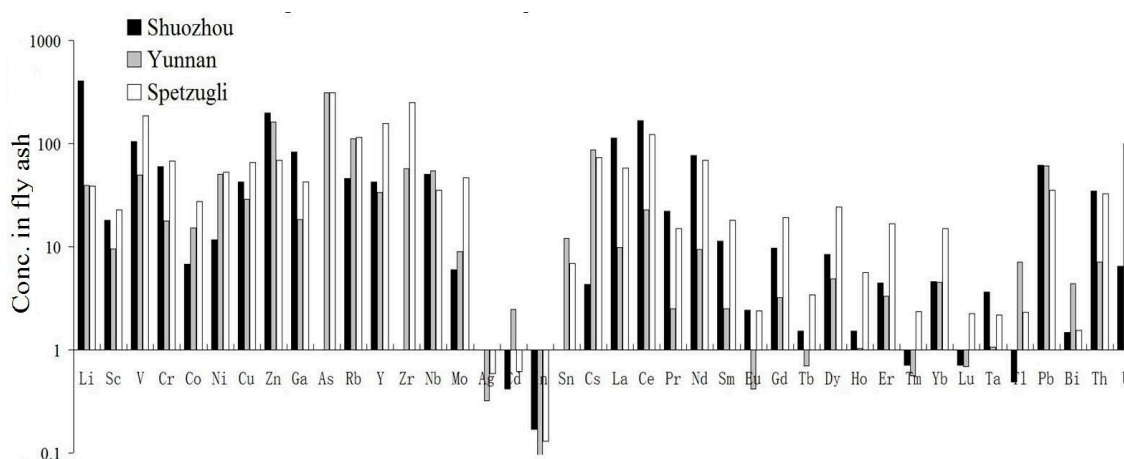


**Figure 2.** Relative concentrations of a number of trace elements in fly ash in Shuozhou, Yunnan, and Spetzugli.

In the present study, CFA was pretreated using desilication to disrupt silicon-aluminum bonds and increase the extraction efficiency of lithium and aluminum during acid leaching. As shown in Figure 3, the complete aluminum and lithium extraction process consists of pre-desilication, intensified acid leaching, filtration, decontamination, and precipitation recycling. The present study focused on the pressure acid leaching of lithium and aluminum from CFA in a hydrochloric acid solution.

The effects of leaching process conditions on lithium and aluminum extraction were systematically investigated, and the correlative mechanisms were characterized.

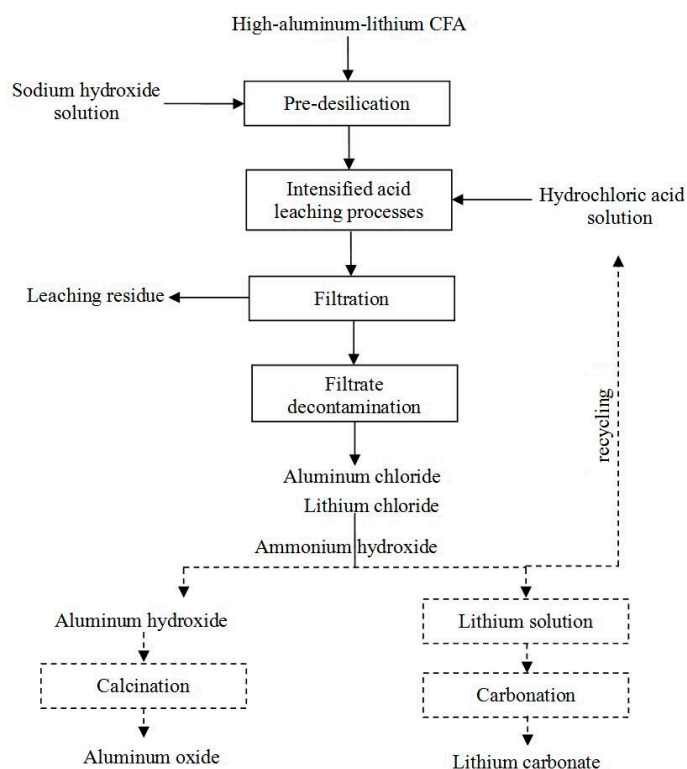


**Figure 3.** A flow diagram of the extraction of aluminum and lithium from coal fly ash (CFA).

## 2. Materials and Methods

### 2.1. Raw Materials

CFA was obtained from the pulverized-coal-fired boilers of thermal power plants in Shuozhou, Shanxi Province, China. The material samples had an average particle size of  $33.2\ \mu\text{m}$  ( $d_{50}$ ) and a  $d_{90}$  value of about  $73.9\ \mu\text{m}$ . The chemical composition of the CFA was analyzed using X-ray fluorescence (XRF) spectroscopy (ARL Perform' X 4200, Thermo Scientific, Boston, MA, USA). Inductively-coupled plasma mass spectrometry (ICP-MS; X Series 2, Thermo Scientific, Boston, MA, USA) was used for the elemental analysis. The morphology and phase mineralogy analyses were carried out using scanning electron microscopy (SEM; UHR FE-SEM SU8220, Hitachi, Japan) and X-ray diffractometry (XRD; D/Max-2200, Rigaku, Japan), respectively.

All the reagents used in this study were of analytical grade, except for HCl,  $\text{H}_2\text{SO}_4$ , HF, and  $\text{HNO}_3$ , which were of guaranteed reagent grade. Deionized water was used for all of the experiments. All of the chemicals were purchased from commercial sources and used as received without further purification.

### 2.2. Pre-Desilication Experiments

The experiments were carried out in a 1 L batch autoclave fitted with a stirring device and external electrical heater system. Typically, a CFA sample (0.2 kg) and a sodium hydroxide solution ( $6 \times 10^{-4}\ \text{m}^3$ ,  $150\ \text{kg}/\text{m}^3$ ) were mixed at a moderate agitation speed at  $120\ ^\circ\text{C}$  for 1 h. The stirring speed of 300 rpm was applied to keep the CFA in suspension for all of the experiments. The selective leaching of amorphous silicon was achieved. After alkaline leaching, the desiliconized CFA (DCFA) was separated from the solution by vacuum filtration. Deionized water was used to remove all of the

residual liquor and increase the final volume to 1 L. The chemical composition of CFA and DCFA are shown in Table 1. The separated DCFA samples were used in the intensified acid leaching processes.

**Table 1.** Main chemical composition of CFA and the desiliconized coal fly ash (DCFA) samples (mass fraction, wt %). Abbreviation: L.O.I, loss of ignition.

Content/%	SiO <sub>2</sub>	Al <sub>2</sub> O <sub>3</sub>	CaO	Fe <sub>2</sub> O <sub>3</sub>	TiO <sub>2</sub>	P <sub>2</sub> O <sub>5</sub>	MgO	Li <sub>2</sub> O	Na <sub>2</sub> O	MnO	L.O.I
CFA	44.12	42.17	2.44	2.43	1.67	0.69	0.68	0.20	0.14	0.02	1.41
DCFA	34.30	49.88	1.98	3.07	1.81	0.08	0.81	0.22	8.74	0.02	0.22

### 2.3. Intensified Acid Leaching Processes

The main objective of the present study was to improve the leaching of aluminum and lithium from CFA, thereby facilitating the downstream recovery of solid aluminum and lithium products. The acid leaching experiments were conducted in 0.5 L sealed hydrothermal reaction kettles fitted with polytetrafluoroethylene-lined pots. These kettles were placed into an incubator heated to the target temperature. The examined acid leaching variables were the acid species, acid concentration, temperature, solid to liquid (S/L) ratio, and time (Table 2). The aluminum in the filtrates was analyzed as detailed in the Chinese national standard GB/T9734-2008; the lithium was analyzed using atomic absorption spectrometry (AAS; Zeenit 700, Analytik Jena AG, Germany). The air-dried residues were analyzed using XRD and SEM. Intensified acid leaching experiments were carried out for both CFA and DCFA.

**Table 2.** Intensified acid leaching conditions. Abbreviations: S/L, solid to liquid.

Factors	Leaching Condition			
	Acid Concentration (mol/L)	Leaching Temperature (°C)	S/L Ratio	Leaching Time (h)
Acid species	6	120	1:20	4
Acid concentration	1, 2, 4, 6, 8	120	1:20	4
Temperature	6	30, 60, 90, 120, 150	1:20	4
S/L ratio	6	120	1:5, 1:10, 1:15, 1:20, 1:30, 1:40	4
Time	6	120	1:20	0.5, 1, 2, 4, 6, 8

## 3. Results and Discussion

### 3.1. CFA Analysis

The chemical composition analysis showed that the CFA samples contained 42.17 wt % aluminum and 0.2 wt % lithium oxide (Table 1), which is equivalent to mid-grade bauxite ores. The combined aluminum and silica content in the CFA was more than 85%, and the mass ratio of aluminum to silicon dioxide (A/S) was approximately 1; thus, the Bayer process is not suitable for the direct recovery of the CFA. However, the concentration of lithium is unusually high in the studied CFA, and close to that of some lithium-rich ores.

The XRD analysis (Figure 4) indicated that the CFA was primarily composed of mullite, corundum, and quartz, which is consistent with previously reported research [14]. Moreover, the lithium phase consisted of minor lithium silicate. SEM images show that the granular features of the CFA consisted of microspherical beads, some of which were smooth, while others were pitted with cracks and subsidence holes. The loss of ignition (L.O.I) of the CFA was determined to be 2.13, which accounts for carbon residue and indicates that some compositions were readily resolved.

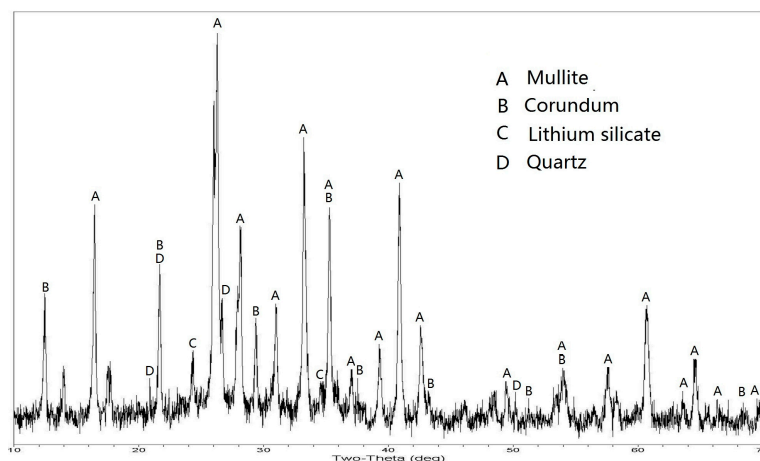


Figure 4. XRD pattern of raw CFA sample.

### 3.2. Pre-Desilication of the CFA

The chemical composition and XRD pattern of the DCFA samples are shown in Table 1 and Figure 5, respectively. After pre-desilication, the A/S ratio of the DCFA increased to 1.5. During the alkali reaction, the free silica was removed from the main phase. However, most mullite and corundum is stable in concentrated sodium hydroxide solution, as shown in Table 3. After pretreatment, lithium silicate was still evident in the XRD pattern. Hydroxy sodalite was produced by the reaction of excess alkali with mullite. Some of the corundum diffraction peaks disappeared after pretreatment; however, very little aluminum could be detected in the alkali leaching solution. Hence, complex chemistry involving corundum and NaOH may have resulted in the formation of  $\text{NaAlO}_2$ , which then reacted with  $\text{Na}_2\text{SiO}_3$  to generate hydroxy sodalite [20], as per reactions (2) and (4). The  $\text{Na}_2\text{O}$  content of the DCFA was significantly greater than that of CFA, which is consistent with the data shown in Table 1. The possible reactions occurring during pre-desilication are as follows:

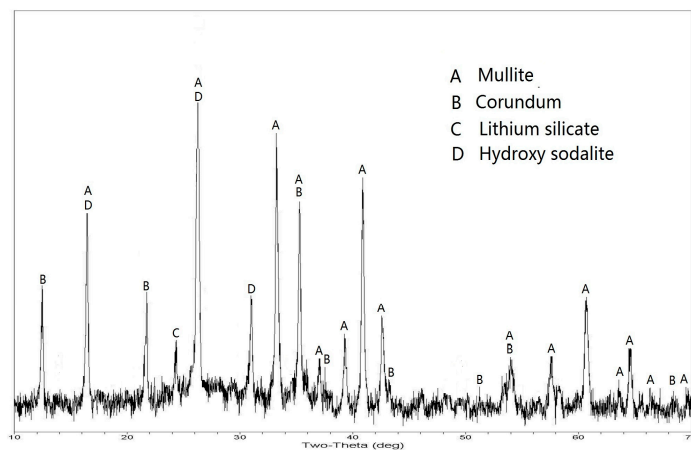
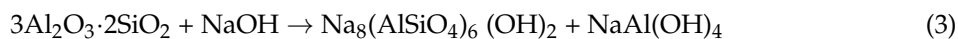
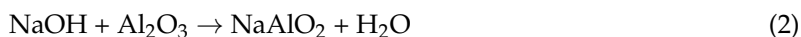
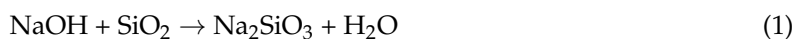


Figure 5. XRD pattern of DCFA.

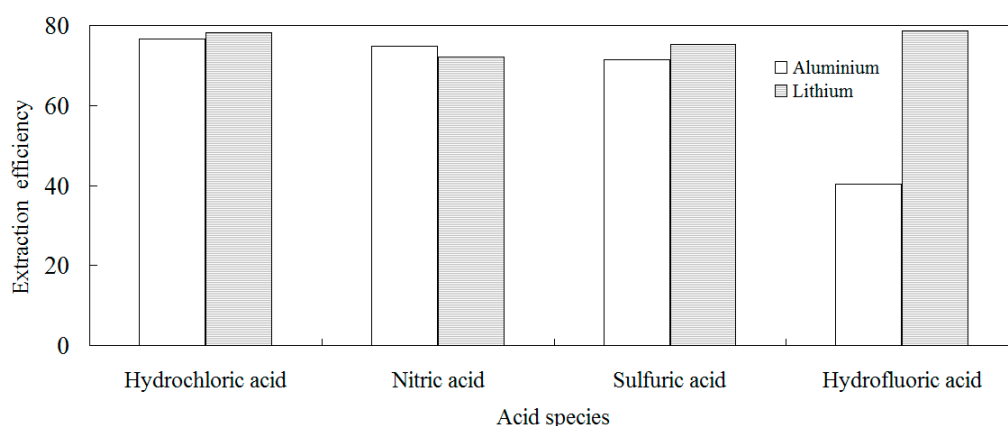
**Table 3.** Mineralogical analysis of CFA and DCFA (wt %).

Phase	Mullite	Quartz	Corundum	Lithium Silicate	Glass Phase	Hydroxy Sodalite	Amphodelite	Calcite
CFA	65.3	3.7	13.2	0.9	12.4	-	-	1.2
DCFA	63.9	2.4	12.1	0.8	-	9.1	2.6	1.6

### 3.3. Intensified Acid Leaching Processes

#### 3.3.1. Effect of Acid Species

The effects of different acid species (hydrochloric acid, nitric acid, sulfuric acid, and hydrofluoric acid) on the leaching rates of aluminum and lithium are shown in Figure 6. After intensified acid leaching, most of the components of the DCFA were dissolved. All of the acids accelerated the pressured leaching of aluminum and lithium. However, hydrofluoric acid exhibited the lowest aluminum and lithium extraction efficiencies. It may be that aluminum fluoride sediment was formed, which was sparingly soluble in water and the mineral acids, but reacted with silicate; the extraction of lithium from DCFA was higher than that of aluminum. The mullite, corundum, and lithium silicate phases were dissolved into the bulk solution. The non-volatility of sulfuric acid is not conducive to the leaching of liquid concentrate; therefore, the extraction of aluminum using sulfuric acid required higher steam temperatures and pressures than those for the other acids tested. The lithium leaching efficiency of hydrochloric acid was higher than that of nitric acid. Hence, hydrochloric acid was selected as the optimal acid species and used in further experiments.

**Figure 6.** Effects of different acid species on the acid leaching of DCFA (6 mol/L, 120 °C, S/L ratio of 1/20, 4 h).

#### 3.3.2. Effect of Hydrochloric Acid Concentration

Hydrochloric acid concentration has a significant effect on the leaching rates of lithium and aluminum [16]. Figure 7 shows that the aluminum and lithium extraction efficiencies increased with hydrochloric acid concentration from 1 to 8 mol/L, with maximal rates of 79.5% and 83.6%, respectively. At higher concentrations, the extraction efficiencies decreased; this was attributed to the mass transfer resistance of aluminum and lithium ions and the resistance of some phases to decomposition as a result of the formation of silicic acid from  $\text{SiO}_3^{2-}$  and  $\text{H}^+$ . The lithium content of DCFA is lower than that of aluminum, and the extraction of aluminum is more efficient than that of lithium. This corresponds with the low observed concentrations of lithium, which does not diffuse well in acidic solutions. Subsequently, a dynamic experimental analysis of lithium leaching was conducted. The aluminum and lithium extraction efficiencies obtained in the present study were higher than those obtained in previous acid leaching studies [16,21] under the same condition. This was attributed to the desilication process and the high-pressure conditions. The results indicate that the optimum hydrochloric acid

concentration was 6 mol/L. Slightly higher extraction efficiencies were obtained with 8 mol/L HCl; however, using 6 mol/L HCl significantly reduces the acid's consumption and pollution.

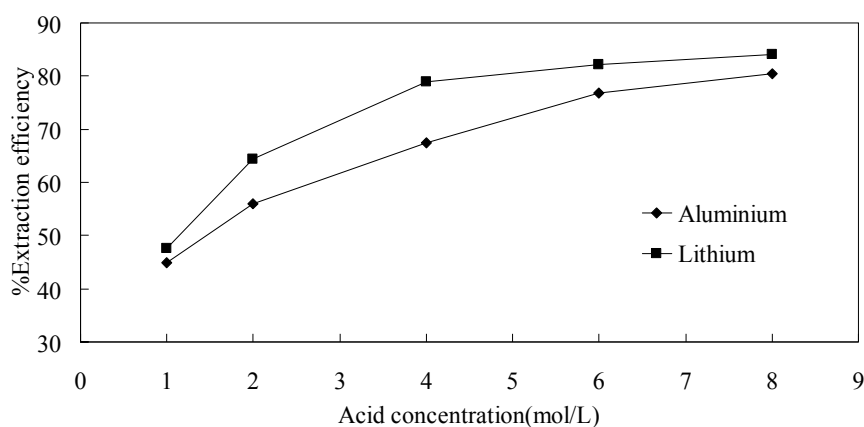


**Figure 7.** Effect of hydrochloric acid concentration on the acid leaching of DCFA (120 °C, S/L ratio of 1/20, 4 h).

### 3.3.3. Effect of Temperature

The effects of temperature on the hydrochloric acid leaching extraction efficiencies of aluminum and lithium from DCFA in a sealed hydrothermal reaction kettle are shown in Figure 8. The aluminum and lithium extraction increased with temperature. At 120 °C, the aluminum and lithium extraction efficiencies were 76.7% and 82.3%, respectively, which were maintained at higher temperatures. At 30 °C, the aluminum and lithium extraction efficiencies were 38.2% and 41.1%, respectively. At approximately 103 °C, the extraction efficiency of aluminum was higher than that of lithium. With increasing temperature and pressure, the diffusion velocities of hydrochloric acid and activated molecules increases rapidly, resulting in higher ion collision probabilities, which increases the rate and effectiveness of leaching. Above 120 °C, the extraction efficiency of aluminum was higher than that of lithium, which was attributed to the low concentration of lithium and its mass transfer resistance. In addition, it is difficult to destroy the mullite structure at low temperatures, and some of the leavings were not dissolved. Considering extraction efficiency and energy consumption, the optimal leaching temperature is 120 °C.

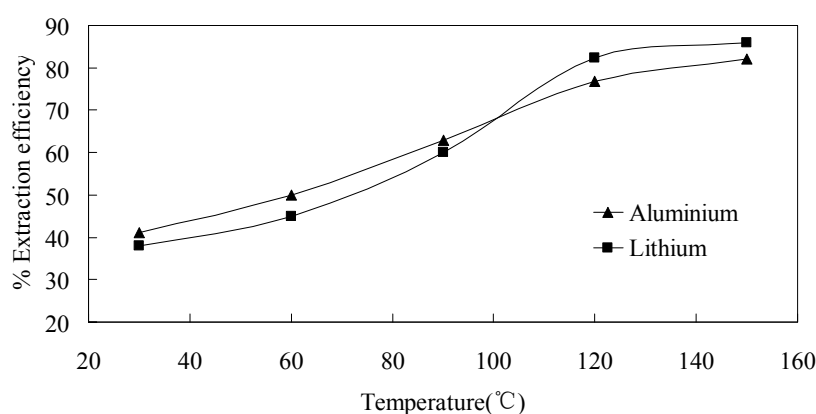


**Figure 8.** Effect of temperature on the acid leaching of DCFA (6 mol/L HCl, S/L ratio of 1/20, 4 h).

### 3.3.4. Effect of S/L Ratio

The leaching experiments were carried out under the following conditions: hydrochloric acid concentration = 6 mol/L, temperature = 120 °C, time = 4 h. The effect of the S/L ratio is shown in Figure 9. The aluminum extraction efficiency decreased from 76.7% to 22% when the S/L was



increased from 1/40 to 1/5. The lithium extraction efficiency decreased linearly when the S/L ratio was decreased from 1/20 to 1/5. The S/L ratio refers to the mass of solids to the volume of acid; the volume of acid is relative, and the mass of solids is constant. Increased acid volume enhances the leaching conditions, and ensures that the DCFA can be thoroughly mixed in the hydrothermal reaction kettle. Violent chemical reactions occurred in the heterogeneous systems when the surfaces of the reactant particles were covered with hydrochloric acid solution, which promoted aluminum and lithium dissolution. Furthermore, the presence of more hydronium ions implies an increased accumulation of silicic acid, which increases the viscosity of the leach liquor, such that it obstructs the mass transfer of lithium and results in lower extraction efficiency. This corresponds with the decrease in lithium extraction efficiency observed at S/L ratios greater than 1/20. Hence, the optimal S/L ratio was determined to be 1/20.

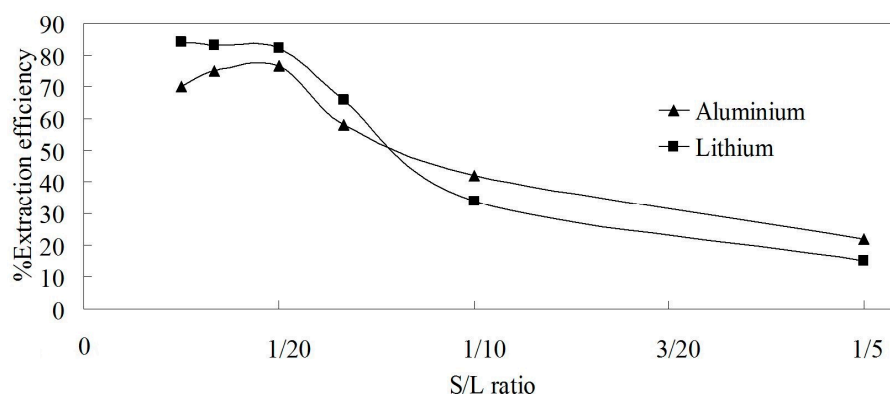


Figure 9. Effect of S/L ratio on the acid leaching of DCFA (6 mol/L HCl, 120 °C, 4 h).

### 3.3.5. Effect of Time

The effects of time on lithium and aluminum extraction efficiencies are depicted in Figure 10. In general, previous studies have indicated that the extraction ratio of aluminum increases with increasing reaction time in acid leaching conditions. A similar trend was observed in the present study. An aluminum extraction efficiency of 36.6%, 76.8%, 78.5%, and 79.5% were obtained after 1 h, 4 h, 6 h, and 8 h of acid leaching, respectively. The lithium extraction efficiency did not significantly increase at acid leaching reaction times longer than 4 h. As the reaction progresses, the aluminum and lithium phases are gradually dissolved, and the reaction substrates become depleted. The decrease in the lithium extraction ratio at long reaction times may be attributed to the production of orthosilicic acid, and the degradation of the lixivium filtering behavior. Thus, optimal aluminum and lithium extraction was achieved after 4 h at a reaction temperature of 120 °C.

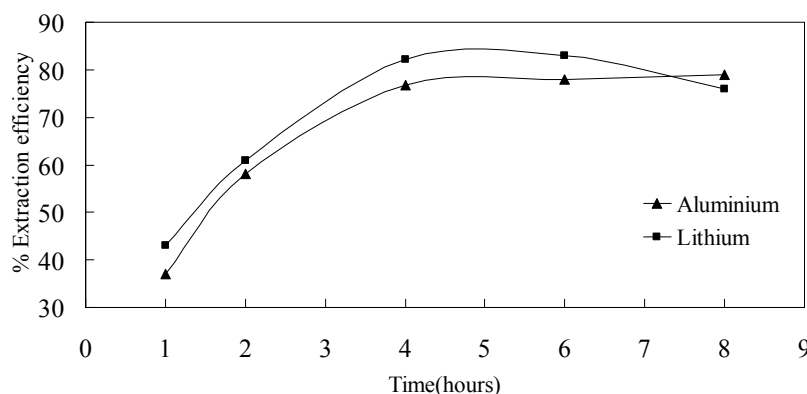


Figure 10. Effect of time on the acid leaching of DCFA (6 mol/L HCl, 120 °C, S/L ratio of 1/20).



### 3.4. Characterization of Lithium and Aluminum Extraction under Optimum Conditions

#### 3.4.1. Extraction Efficiency of Lithium and Aluminum from CFA and DCFA

The novel recovery process developed in the present study consisted of pre-desilication and intensified acid leaching. The single factor experiments resulted in the following optimized acid leaching conditions for extracting aluminum from DCFA: a hydrochloric acid concentration of 6 mol/L, a leaching temperature of 120 °C, pressure of 1.8 MPa, an S/L ratio of 1/20, and a leaching time of 4 h. Figure 11 shows the lithium and aluminum extraction efficiencies for CFA and DCFA under these optimized conditions. The extraction ratios of lithium and aluminum from the DCFA nearly doubled after 4 h. Figure 11a indicates that the CFA desilication process enhances the leaching of lithium. The lithium extraction efficiency of CFA is similar to that of DCFA in the initial stage of pressure acid leaching. However, the amount of lithium extracted from the DCFA increases dramatically during the latter leaching stage. For DCFA, 82.3% of the total lithium was extracted at 4 h, which then decreased slowly with increased leaching time; the lithium extraction from CFA increased slowly with time. Figure 11b compares the aluminum extraction efficiencies from CFA and DCFA under the same conditions (10 g, 120 °C, 6 mol/L HCl, 1/20 S/L ratio, in a sealed hydrothermal reaction kettle). The aluminum extraction efficiency increased with leaching time for both CFA and DCFA. The aluminum extraction ratio of DCFA was significantly higher than that of CFA after 10 min. This result indicates that a significant proportion of the mullite, which is highly stable and acid-resistant, was dissolved or transformed into soluble substances. In the pre-desilication and intensified acid leaching processes, the sodium hydroxide and hydrochloric acid are present in excess, based upon stoichiometric calculations; thus, the lithium and aluminum could theoretically be completely leached out. During the desilication stage, sodium aluminate was generated from the excess alkali, and transformed into aluminum hydroxide. This was dissolved under acidic conditions, which resulted in a rapid increase in aluminum extraction during the early acid leaching stage. The results show that the leaching reaction rate may be controlled by chemical reactions and diffusion mass transfer at the early stage of acid leaching, and that the extraction of aluminum occurred mainly via chemical reactions; lithium extraction was mainly controlled by diffusion mass transfer in the later stages of leaching. This agrees with the results of previous work [26]. Hence, the desilication of CFA is feasible and necessary for the efficient extraction of lithium and aluminum. However, as is shown in Table 4, the main chemical compositions distribution of CFA, DCFA, and the residues demonstrates that most of the lithium and aluminum in the DCFA was dissolved with the intensified acid leaching.

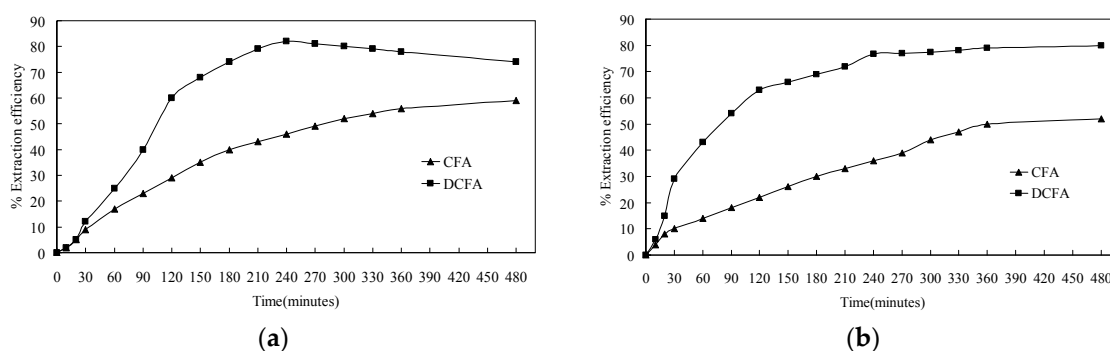


**Figure 11.** Extraction efficiency of CFA and DCFA under optimum conditions, (a) lithium extraction; (b) aluminum extraction (6 mol/L, 120 °C, S/L ratio of 1/20, 4 h).

**Table 4.** Chemical compositions of CFA, DCFA, and the residues (mass fraction, wt %).

Content/%	SiO <sub>2</sub>	Al <sub>2</sub> O <sub>3</sub>	CaO	Fe <sub>2</sub> O <sub>3</sub>	TiO <sub>2</sub>	MgO	Li <sub>2</sub> O
CFA	44.12	42.17	2.44	2.43	1.67	0.68	0.20
DCFA	34.30	49.88	1.98	3.07	1.81	0.81	0.22
Leaching residue	76.81	9.84	0.31	0.26	1.31	0.12	0.02

### 3.4.2. Morphological Analysis

Representative samples processed under different conditions were prepared and examined using SEM. Figure 12 shows the microscopic surface topographies of CFA, DCFA, and the acid leaching residue. Glazed microspheres and spongy porous bodies can be clearly seen in the CFA sample (Figure 12a). The major components of these microspheres were found to be aluminum oxide and silicon dioxide, which corresponds to the results of previous studies [20]. Generally, cenospheres are smaller and darker than ferrospheres. After the desilication of the CFA, the surfaces of the microspheres become coarse and collapsed, and the main components were gradually eroded (Figure 12b). This was beneficial for the transport of acid ions into the interiors of the large irregular particles. A majority of the spherical bodies were decomposed, becoming smaller and irregularly shaped (Figure 12c,d). Hydrogen ions reacted with the mullite and corundum to generate small holes, which is also consistent with previous observations [14]. A large quantity of the abundant alumina was dissolved by the acid, as was the lithium silicate. This result is consistent with the observed increase in the extraction efficiencies of lithium and aluminum with time.

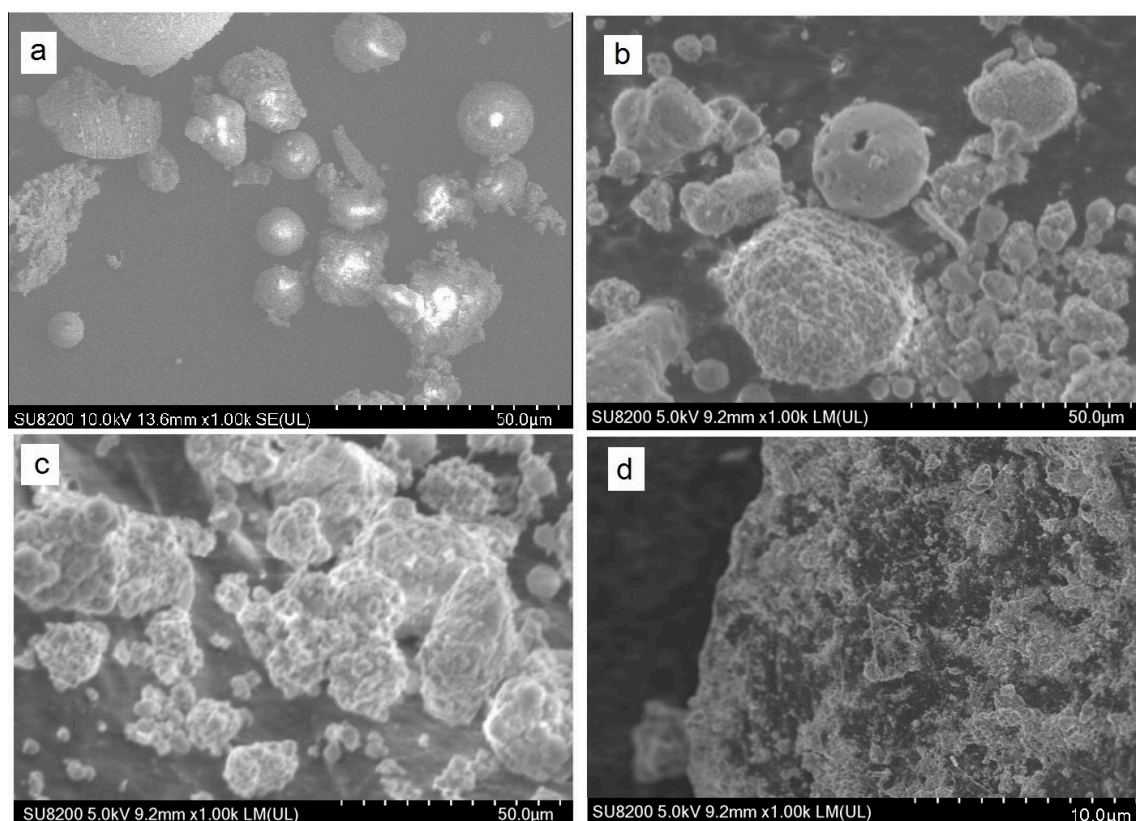


**Figure 12.** SEM images of samples processed under optimum conditions. (a) CFA; (b) DCFA; (c,d) acid leaching residue (6 mol/L HCl, 120 °C, S/L ratio of 1/20, 4 h).

#### 4. Conclusions

In the present study, a two-step process, based on pre-desilication and intensified acid leaching, was developed for the efficient extraction of aluminum and lithium from CFA. The factors influencing the extraction of aluminum and lithium under pressure acid leaching were investigated. The optimal pre-desilication conditions were experimentally determined to be a 150 kg/m<sup>3</sup> sodium hydroxide solution, an S/L ratio of 1/3, a temperature of 120 °C, and a reaction time of 1 h. In the intensified acid leaching process, aluminum and lithium extraction efficiencies of 76.7% and 82.3%, respectively, were obtained from DCFA under optimum acid leaching conditions: a hydrochloric acid concentration of 6 mol/L, a leaching temperature of 120 °C, an S/L ratio of 1/20, and a leaching time of 4 h.

The experimental results show that the A/S ratio of the CFA was increased from 1 to 1.5 after desiliconization. Overall, the extraction ratio of lithium was higher than that of aluminum. Compared with using only acid leaching, the pre-desilication process significantly increased the extraction efficiencies of lithium and aluminum from the CFA. Further studies are needed to assess the viability of recycling process of HCl and the economy, and the separation and purification of lithium and aluminum products will be investigated in the next stage.

**Acknowledgments:** Special thanks are given to the editor and reviewers for their careful reviews. We gratefully acknowledge financial support from the National Natural Science Foundation of China (No. 41472133), the Science Foundation of Hebei (No. D2014402046), and the Scientific Research Foundation of the Higher Education Institutions of Hebei Province (No. QN2016049).

**Author Contributions:** Shenyong Li and Shenjun Qin conceived and designed the experiments; Shenyong Li and Lianwei Kang performed the experiments; Jianjun Liu and Jing Wang analyzed the data; Yanheng Li contributed sample fabrication; Shenyong Li wrote the paper. All authors contributed to the data analysis and discussion.

**Conflicts of Interest:** The authors declare no conflict of interest.

#### References

1. Li, J.F.; Dong, H.; Sun, J.; Nie, J.H.; Zhang, S.Y.; Tang, J.S.; Chen, Z.H. Composition profiles and health risk of PCDD/F in outdoor air and fly ash from municipal solid waste incineration and adjacent villages in East China. *Sci. Total Environ.* **2016**, *571*, 876–882. [[CrossRef](#)] [[PubMed](#)]
2. Meawad, A.S.; Bojinova, D.Y.; Pelovski, Y.G. Review: An overview of metals recovery from thermal power plant solid wastes. *Waste Manag.* **2010**, *30*, 2548–2559. [[CrossRef](#)] [[PubMed](#)]
3. Silva, L.F.; DaBoit, K.; Sampaio, C.H.; Jasper, A.; Andrade, M.L.; Kostova, I.J.; Waanders, F.B.; Henke, K.R.; Hower, J.C. The occurrence of hazardous volatile elements and nanoparticles in Bulgarian coal fly ashes and the effect on human health exposure. *Sci. Total Environ.* **2012**, *416*, 513–526. [[CrossRef](#)] [[PubMed](#)]
4. Komonweeraket, K.; Cetin, B.; Benson, C.H.; Aydılek, A.H.; Edil, T.B. Leaching characteristics of toxic constituents from coal fly ash mixed soils under the influence of pH. *Waste Manag.* **2015**, *38*, 174–184. [[CrossRef](#)] [[PubMed](#)]
5. Qin, S.J.; Sun, Y.Z.; Li, Y.H.; Wang, J.X.; Zhao, C.L.; Gao, K. Coal deposits as promising alternative sources for gallium. *Earth-Sci. Rev.* **2015**, *150*, 95–101. [[CrossRef](#)]
6. Sun, J.M.; Zhang, Z.J.; Chen, G.; Yan, S.Y.; Huo, Q.Z.; Wu, L.C.; Xu, H.L.; Qin, L.; Chen, X.X. Method for Co-Producing Alumina and Activated Calcium Silicate from High-Alumina Fly Ash. U.S. Patent 9,139,445, 22 September 2015.
7. Dai, S.F.; Zhao, L.; Peng, S.P.; Chou, C.L.; Wang, X.B.; Zhang, Y.; Li, D.; Sun, Y.Y. Abundances and distribution of minerals and elements in high-aluminum coal fly ash from the Jungar Power Plant, Inner Mongolia, China. *Int. J. Coal Geol.* **2010**, *81*, 320–332. [[CrossRef](#)]
8. Sun, Y.Z.; Zhao, C.L.; Qin, S.J.; Xiao, L.; Li, Z.S.; Lin, M.Y. Occurrence of some valuable elements in the unique ‘high-aluminium coals’ from the Jungar coalfield, China. *Ore Geol. Rev.* **2016**, *72*, 659–668. [[CrossRef](#)]
9. Dai, S.F.; Zhao, L.; Hower, J.C.; Johnston, M.N.; Song, W.J.; Wang, P.P.; Zhang, S.F. Petrology, mineralogy, and chemistry of size-fractioned fly ash from the Jungar power plant, Inner Mongolia, China, with emphasis on the distribution of rare earth elements. *Energy Fuels* **2014**, *28*, 1502–1514. [[CrossRef](#)]
10. Wang, J.X.; Wang, Q.; Tian, L. Characteristics of trace elements of the No. 9 coal seam from the Anjialing Mine, Ningwu coalfield, China. *Chin. J. Geochem.* **2015**, *34*, 391–400.

11. Dai, S.F.; Seredin, V.V.; Ward, C.R.; Jiang, J.H.; Hower, J.C.; Song, X.L.; Jiang, Y.F.; Wang, X.B.; Gornostaeva, T.; Li, X.; et al. Composition and modes of occurrence of minerals and elements in coal combustion products derived from high-Ge coals. *Int. J. Coal Geol.* **2014**, *121*, 79–97. [[CrossRef](#)]
12. Qin, S.J.; Zhao, C.L.; Li, Y.H.; Zhang, Y. Review of coal as a promising source of lithium. *Int. J. Oil Gas Coal Technol.* **2015**, *9*, 215–229. [[CrossRef](#)]
13. Shemi, A.; Mpana, R.N.; Ndlovu, S.; Dyk, L.D.; Sibanda, V.; Seepe, L. Alternative techniques for extracting aluminum from coal fly ash. *Miner. Eng.* **2012**, *34*, 30–37. [[CrossRef](#)]
14. Xu, D.H.; Li, H.Q.; Bao, W.J.; Wang, C.Y. A new process of extracting aluminum from high-aluminum coal fly ash in  $\text{NH}_4\text{HSO}_4 + \text{H}_2\text{SO}_4$  mixed solution. *Hydrometallurgy* **2016**, *165*, 336–344. [[CrossRef](#)]
15. Shemi, A.; Ndlovu, S.; Sibanda, V.; Dyk, L.D. Extraction of aluminum from coal fly ash using an acid leach-sinter-acid leach technique. *Hydrometallurgy* **2015**, *157*, 348–355. [[CrossRef](#)]
16. Izquierdo, M.; Koukoulas, N.; Toulou, S.; Panopoulos, K.D.; Querol, X.; Itskos, G. Geochemical controls on leaching of lignite-fired combustion by-products from Greece. *Appl. Geochem.* **2011**, *26*, 1599–1606. [[CrossRef](#)]
17. Li, G.H.; You, Z.X.; Sun, H.; Sun, R.; Peng, Z.W.; Zhang, Y.B.; Jiang, T. Separation of rhenium from lead-rich molybdenite concentrate via hydrochloric acid leaching followed by oxidative roasting. *Metals* **2016**, *6*, 282. [[CrossRef](#)]
18. Tripathy, A.K.; Sarangi, C.K.; Tripathy, B.C.; Sanjay, K.; Bhattacharya, I.N.; Mahapatra, B.K.; Behera, P.K.; Satpathy, B.K. Aluminum recovery from NALCO fly ash by acid digestion in the presence of fluoride ion. *Int. J. Miner. Process.* **2015**, *138*, 44–48. [[CrossRef](#)]
19. Zhang, R.; Zheng, S.L.; Ma, S.H.; Zhang, Y. Recovery of alumina and alkali in Bayer red mud by the formation of andradite-grossular hydrogarnet in hydrothermal process. *J. Hazard. Mater.* **2011**, *189*, 827–835. [[CrossRef](#)] [[PubMed](#)]
20. Li, H.Q.; Hui, J.B.; Wang, C.Y.; Bao, W.J.; Sun, Z.H. Extraction of alumina from coal fly ash by mixed-alkaline hydrothermal method. *Hydrometallurgy* **2014**, *147–148*, 183–187. [[CrossRef](#)]
21. Ding, J.; Ma, S.H.; Zheng, S.L.; Zhang, Y.; Xie, Z.L.; Shen, S.; Liu, Z.K. Study of extracting alumina from high-alumina PC fly ash by a hydro-chemical process. *Hydrometallurgy* **2016**, *161*, 58–64. [[CrossRef](#)]
22. Matjie, R.H.; Bunt, J.R.; Heerden, J.H.P. Extraction of aluminum from coal fly ash generated from a selected low rank bituminous South African coal. *Miner. Eng.* **2005**, *18*, 299–310. [[CrossRef](#)]
23. Bai, G.H.; Teng, W.; Wang, X.G.; Qin, J.G.; Xu, P.; Li, P.C. Alkali desilicated coal fly ash as substitute of bauxite in lime-soda sintering process for aluminum production. *Trans. Nonferr. Met. Soc. China* **2010**, *20*, 169–175. [[CrossRef](#)]
24. Li, L.S.; Liao, X.Q.; Wu, Y.S.; Liu, Y.Y. Extracting aluminum from coal fly ash with ammonium sulfate sintering process. In *Light Metals*; Springer: New York, NY, USA, 2012; Volume 510, pp. 213–217.
25. Vu, H.; Bernardi, J.; Jandová, J.; Vaculíková, L.; Goliáš, V. Lithium and rubidium extraction from zinnwaldite by alkali digestion process: Sintering mechanism and leaching kinetics. *Int. J. Miner. Process.* **2013**, *123*, 9–17. [[CrossRef](#)]
26. Yao, Z.T.; Xia, M.S.; Sarker, P.K.; Chen, T. A review of the aluminum recovery from coal fly ash, with a focus in China. *Fuel* **2014**, *120*, 74–85. [[CrossRef](#)]

